A VIRTUAL DESIGN METHODOLOGY TO IMPROVE THE DYNAMICS AND PRODUCTIVITY OF LARGE MILLING TOOLS

M. Etxebeste[a*], G. Ortiz-de-Zarate[a], I.M. Arrieta[a], P. J. Arrazola[a]

[a] Mondragon Unibertsitatea, Faculty of Engineering, Loramendi 4, Arrasate-Mondragón, 20500, Spain
* Corresponding author. E-mail address: metxebeste@mondragon.edu

Abstract

Large cutting tools are widely used in sectors such as automotive, where complex shape aluminium components are machined at high cutting speeds, in a single clamping and in short cycle times with elevated Material Removal Rate (MRR). However, their relatively low stiffness and natural frequencies make chatter the primary productivity limitation. Developing optimised tools to overcome these limitations is often cost-prohibitive with current design methods. This paper presents a virtual design methodology for optimising large milling tools to mitigate chatter through topology optimisation and Finite Element Modal Analysis (FEMA). Topology optimisation enhanced tool dynamics, enabling chatter reduction under higher productivity conditions. An improved FEMA model was developed to accurately predict the modal parameters of the cutting tools, featuring a high-fidelity representation of the tool-holder clamping to the spindle. The predicted modal parameters enable cost-effective chatter prediction for tool design validations, minimising development and experimental costs. To validate the methodology, a prototype of the optimised tool was manufactured and tested through experimental modal analysis and machining tests, demonstrating significant productivity improvement in MRR compared to the initial design.

Keywords:

Milling

Chatter suppression

Cutting tool dynamics

Topology optimisation

Virtual design

FEMA

Automotive

1. Introduction

Cutting tool design is critical when large-sized customised tools are required to meet stringent productivity, tolerances, and surface finish demands in challenging applications such as high-speed milling [1], [2]. In recent years, the automotive sector has seen a significant increase in the use of large milling tools, driven by the growing demand for e-mobility components like electric motor housings and battery trays [2]. This trend has led to the adoption of tools with larger diameters or extended lengths, allowing machining in a single clamping [1], [2]. These components, typically made from aluminium alloys, are machined at high cutting speeds [3], which imposes additional demands on the performance of large milling tools.

In milling processes dynamic aspects become critical when using large tools with high mass and relatively low stiffness [1], [4]. These limitations can restrict process productivity and necessitate optimised tool designs to enhance machining performance. Furthermore, the excessive weight of large tools can lead to spindle bearing damage, automatic tool changing issues, reduced maximum spindle speed, and inaccuracies in the final part [1], [4], [5]. For tools with high dynamic flexibility, chatter is usually the main factor limiting Material Removal Rate (MRR) [6]. If chatter occurs during machining, the operation cannot be completed due to factors such as unacceptable inaccuracies and surface finishes, excessive noise, potential damage to the machine-tool, and premature cutting insert breakages [6], [7].

Chatter is commonly analysed via Stability Lobe Diagrams (SLD), which are used to evaluate the dynamic behaviour of a machining system and select chatter free cutting conditions [4], [7], [8], [9]. SLDs delineate stable and unstable machining regions, typically based on depth of cut (a_p) and spindle speed (S). Other cutting parameters can also be considered, and even 3D SLDs can be constructed by incorporating additional influential variables, such as tool overhang length [10]. The procedure to obtain SLD is described in Figure 1. They are determined using four main input parameters [7]: (i) cutting forces (from specific cutting forces, K_s), (ii) machining system dynamics, including modal parameters of the cutting tool: stiffness (k), natural frequency (ω_n), and damping ratio (ζ), (iii) process parameters, and (iv) cutting tool geometry such as number of teeth (z) and diameter ($Ø$). Based on these inputs, SLDs can be calculated using time-domain and frequency-domain models [8], [11]. Of these, the frequency-domain models of Average Tooth and Fourier Series models can be said to offer a superior balance between accuracy and computational cost [8]. However, time-domain models may prove more accurate for complex geometries [7], [8]. Therefore, to efficiently predict chatter, the optimal approach must be determined for each machining process, and the input parameters must be accurately defined.

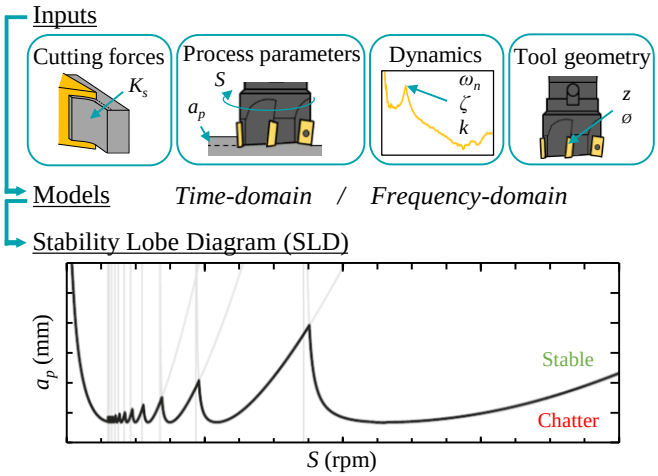

Figure 1: Procedure to obtain SLD.

The input parameters for calculating SLDs include process parameters and cutting tool geometry, both defined by the machining process [7]. Cutting forces can be determined using mathematical models that are fed by specific cutting forces [7], [12], [13]. The specific cutting force is primarily influenced by the workpiece material; however, other parameters such as cutting geometry and cutting conditions can also have a significant influence [3], [12]. Specific cutting forces in milling processes can be obtained experimentally by correlating measured cutting forces with the chip area from milling tests, or by transforming outputs from orthogonal cutting tests to oblique tool geometry [3]. They can also be predicted using empirical [3], Finite Element Method (FEM) [14], analytical [15], and hybrid models [16]. Among them, Lazkano et al. [3] developed one of the most relevant specific cutting force databases for A-356 alloy considering the influence of most relevant parameters.

Another input to consider in the prediction of chatter is the machining system dynamics [6]. In the case of large cutting tools, the modal parameters of the cutting tool set need to be obtained from the critical vibration mode [6], [17], [18]. Tool-tip modal parameters can be obtained from the Frequency Response Function (FRF) measured through Experimental Modal Analysis (EMA), usually via tap testing [4], [6], [7]. Nevertheless, to perform EMA in the design of new cutting tools, each tool design must be produced, which is costly and impractical, particularly for large cutting tools. Therefore, both analytical and Finite Element Modal Analysis (FEMA) models have been developed to predict cutting tool's modal parameters.

Analytical models, usually based on Euler-Bernoulli and Timoshenko beam models, are computationally efficient and suitable for simple geometries [7], [8]. The Receptance Coupling Substructure Analysis (RCSA) method stands out as one of

the most relevant analytical methods due to its ability to predict the tool-tip response by considering the entire cutting tool and spindle system [8], [10], [19]. RCSA couples the modelled receptances of tools and holders with measured spindle-machine receptances to predict tool-tip receptances, delivering accurate results that account for multiple vibration modes [8], [20]. This approach has been further advanced by incorporating multi-component RCSA analysis with FEM models to model complex geometries [21], [22], and by using multi-point RCSA to enable multiple coupling locations between the tool's external surface inside the holder and the internal surface of the holder that clamps the tool [20]. In addition, inverse RCSA has proven to be effective for mass and damping compensation in accelerometer-based impact testing [23]. RCSA method has been reviewed for milling applications, including tool-holder modelling, connection modelling, spindle-machine receptances, and applications [19]. However, these approaches still require experimental testing, making them unsuitable for a fully virtual method.

FEMA models can predict the modal parameters of cutting tools, even for complex geometries [24]. In these models, the applied boundary conditions and simplifications have a significant impact [24], [25], [26]. Some researchers have developed accurate FEM models that include the spindle to predict FRFs by considering boundary conditions related to spindle bearings and supports [27], [28]. However, these models require high development costs and must be tailored to each specific machine-tool spindle configuration. In large cutting tools, the spindle is typically much stiffer than the tool, and the model can focus on predicting the dominant vibration mode of the cutting tool [6], [17], [18]. FEMA models that focus solely on the cutting tool have been developed using various boundary conditions, even for the same clamping mechanism [24], [25]. Some models constrain displacements at the double-face contact surfaces of HSK-A63 clamping [24], [26], offering a less time-consuming approach, but this may oversimplify the model and reduce accuracy. As clamping appears to be the main influential parameter some researchers have attempted to model the tool clamped to the spindle by applying the clamping force once the tool is assembled [25]. However, this approach, fails to consider the clamping process itself, which involves mechanical forces and deflections in the cutting tool cone. Currently, no validated cost-effective FEMA model for large milling tool have been found that accurately predict modal parameters with realistic boundary conditions identified as the most critical factor in such cases.

After predicting the occurrence of chatter, various strategies can be employed in cutting tools to prevent or suppress vibrations [6], [7]. Chatter suppression strategies are classified as active, semi-active, or passive [7], [9]. Nevertheless, both active and semi-active strategies require external control devices and actuators that are usually not feasible in the case of milling cutting tools [1], [17]. Thus, passive strategies are often the main choice for milling cutting tool solutions, employing devices, methodologies, or techniques to improve machining performance against chatter [7], [9]. Passive strategies include the use of variable cutting geometries, integration of dampers, and optimisation of cutting tool geometry. Variable cutting geometries, such as variable helix angles and tooth pitches, have been developed to disrupt the regenerative effect of chatter and improve stability [29]. In the case of passive dampers, Tuned Mass Dampers (TMDs) have demonstrated efficacy in suppressing chatter in milling tools [17], [29]. These devices comprise a lumped mass with springs and damping elements connected to the cutting tool, usually embedded within the tool [17], [30], [31]. High-damping materials have also been integrated into cutting tools as alternative solutions to suppress vibrations [32]. Although dampers effectively suppress chatter, their use is often limited by space constraints, functional range limitations, added costs, and maintenance concerns. Therefore, for large cutting tools, developing optimised geometries through methodologies such as topology optimisation emerges as an effective solution.

Several authors have proposed topology optimisation for improving the dynamic behaviour of cutting tools [1], [5], [33], [34]. Topology optimisation is especially applicable to large cutting tools, allowing lighter designs while maintaining stiffness [1]. Usually, topology optimisation is integrated with advanced manufacturing techniques, such as additive manufacturing, which offers greater geometric adaptability [35], or hybrid manufacturing, which combines additive and subtractive processes [36]. Tomasoni et al. [35] developed a lightweight milling head with Additive Manufacturing (AM). Möhring et al. [1], combined topology optimisation for weight reduction with magnetorheological fluid to enhance damping in the same cutting tool, achieving reduced tool vibrations, improved surface roughness, and increased MRR. Nonetheless, most studies have mainly focused on weight reduction, with limited attention to dynamic performance despite its critical importance [1], [5]. One exception is Hanzl et al. [37] who developed a topologically optimised milling head with AM improving dynamic response in EMA tests. However, they did not consider chatter analysis or include experimental machining tests.

The literature review revealed the absence of a comprehensive methodology for identifying, predicting, and addressing critical productivity challenges, such as chatter, during the design of optimised large cutting tools. Although, topology optimisation of cutting tools shows great potential to improve machining stability, its feasibility in reducing chatter has not been previously validated. Furthermore, there is a notable lack of validated FEMA models capable of accurately predicting the modal parameters of cutting tools.

In this paper we present a cost-effective virtual design methodology for the optimisation of large cutting tools to improve the dynamics and performance. The proposed methodology combines topology optimisation and improved FEMA models. Topology optimisation improves tool design to mitigate chatter, particularly in applications where other techniques are not feasible. The improved FEMA model enables accurate prediction of modal parameters allowing for chatter prediction and virtual validation of designs without the need for extensive experimental tests. The virtual design methodology was developed and validated through a real case study involving a long milling tool used for high-speed machining of deep pockets in aluminium components for the automotive sector. The optimised design prototype was manufactured to validate the proposed methodology by comparing the initial and optimised designs through experimental tests, including Experimental Modal Analysis (EMA) and machining tests, measuring key outputs to identify chatter.

2. Virtual design methodology

The virtual design methodology enables cost-effective optimisation of large cutting tools to enhance productivity through topology optimisation and modal parameter prediction using FEMA models, allowing dynamic validation of the developed designs without the need for experimental tests. This approach is specifically tailored for large cutting tools, where the cutting tool itself is typically the critical component of the system, with a dominant vibration mode. The methodology focuses on the tool's critical mode for both prediction and optimisation streamlining the design process and significantly reducing development costs. If this methodology were applied to other types of cutting tools, where multiple vibration modes may be significant (e.g., tools with stiffness similar to the spindle), a preliminary analysis would be needed to determine whether cutting tool optimisation could effectively enhance process productivity. The developed virtual design methodology, along with its experimental validation, is illustrated in Figure 2.

This methodology is divided in three main stages of (i) design optimisation, (ii) virtual modal analysis, and (iii) virtual dynamic validation. The optimisation of the initial design starts from defining the optimisation objective considering process constraints such as, machine-tool limitations, cutting tool and workpiece geometry, and machining operation. Then, the initial design is optimised through topology optimisation to achieve the defined objectives considering design constrains (for example the usable length or the maximum diameter). The topologically optimised design must then be redesigned for manufacturing to ensure it can be produced with the selected method (additive, subtractive, or combination of both). Subsequently, the modal analysis of the initial and optimised designs is performed by FEMA models to obtain the stiffness and natural frequency values for dynamic validation. Once the cutting tools are virtually characterised, the dynamic validation of the developed design is performed based on the SLDs. To calculate SLD, other inputs such as specific cutting forces and process parameters needs to be established. In the end, the optimised design is virtually validated by comparing the maximum stable Material Removal Rates ($MRR_{max\ opt.}$ vs. $MRR_{max\ initial}$) identified at a specific axial depth of cut (a_p). This validation criterion is based on the predicted SLDs, which allow for the determination of the maximum stable spindle speed for each design. If the optimised design achieves higher productivity and meets the established objectives, it is approved for manufacture. Otherwise, the design optimisation process is revisited and refined to achieve the desired performance improvements.

Finally, Experimental Modal Analysis (EMA) and machining tests on both the initial and optimised designs were carried out to validate the proposed methodology. Once the models of the methodology are validated, these experimental tests will no longer be necessary. The developed FEMA model was validated by comparing its predicted modal parameters with those obtained from other models and experimental measurement. The dynamic model to predict chatter was validated through experimental machining tests at different cutting conditions of spindle speed (S) and axial depth of cut (a_p), identifying chatter or stable conditions based on experimental outputs: cutting forces, accelerations, sound emissions, and surface finish. In the end, both the optimised cutting tool design and the virtual design methodology used in its development were validated by quantifying the improvements achieved through the design optimisation in experimental tests.

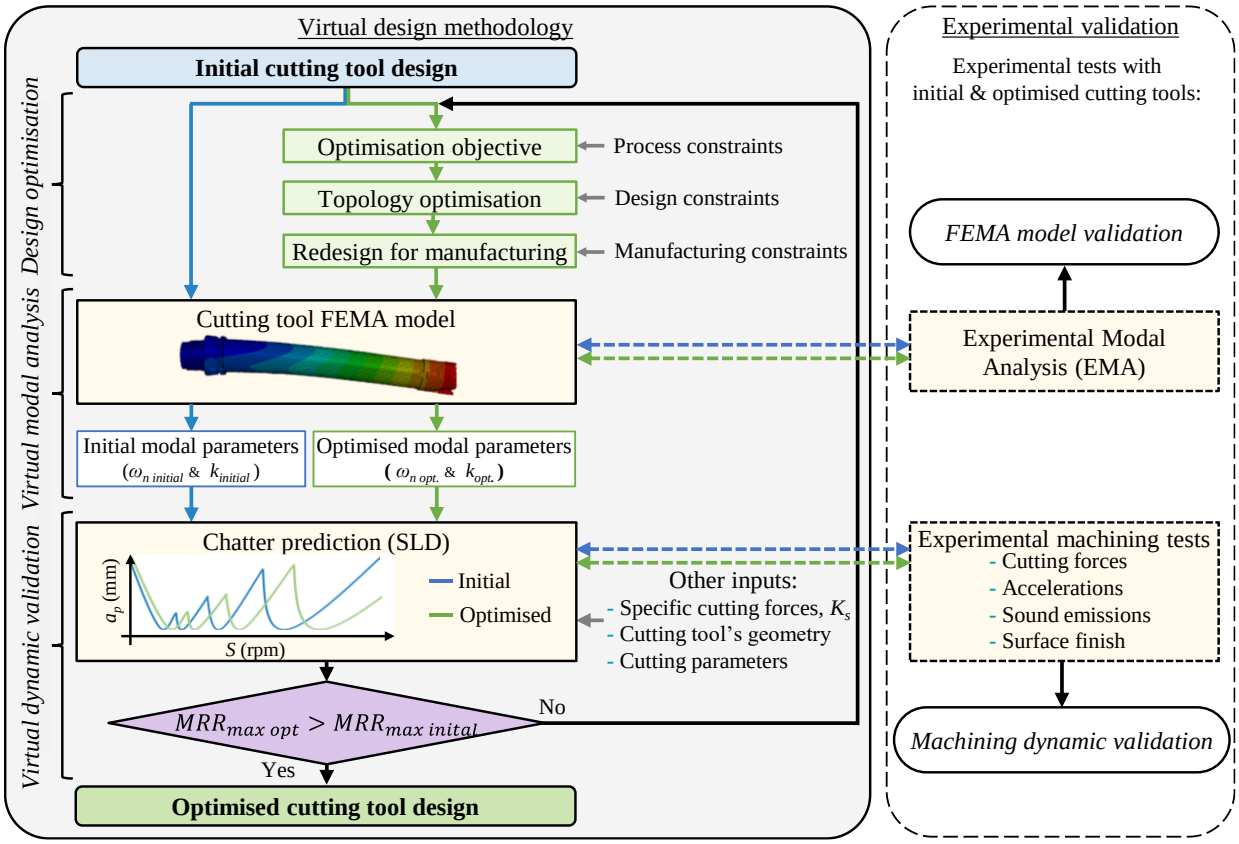

Figure 2: Developed virtual design methodology and its experimental validation process.

3. Virtual design methodology application to a real case study

The proposed virtual design methodology was developed and validated through a real case study involving a long milling tool set used for aluminium machining in automotive sector. This tool was used to machine the deepest part of a stator housing (Figure 3). This operation involves a face milling process to remove a relatively large volume of material in high-speed machining. The required tolerances in this operation are not that tight compared to the rest of the stator housing, making productivity in terms of MRR the main factor to be improved. Geometric tolerances to be achieved in these components are usually 0.05 mm in concentricity, 0.03 mm in perpendicularity and 0.02 mm in circularity [2].

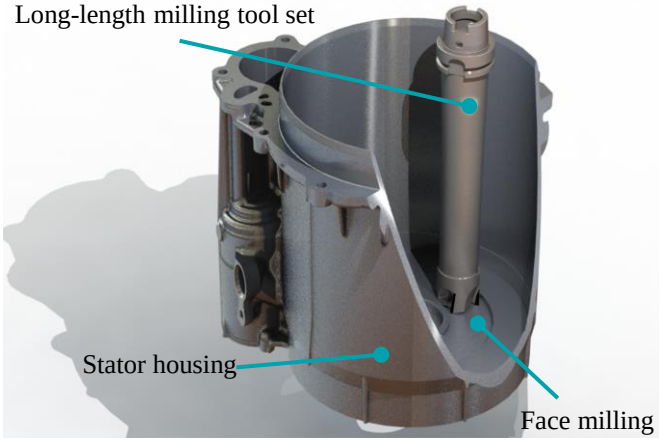

Figure 3: Real case study definition.

In this case, chatter was the main limiting factor of MRR, caused by the relatively low stiffness of the cutting tool. Through the developed methodology, the initial tool geometry was optimised to enhance its dynamic performance. The milling tool set consist of a long tool holder (with HSK-A63 coupling) and a milling head with four teeth ($z = 4$) PCD inserts (Figure 4a). The required cutting tool set length was more than five times the tool diameter $L > 5 \cdot Ø_{tool}$. For the chosen 50 mm milling head, the total projection of the cutting tool from the spindle coupling exceeds 345 mm, which is a considerably long cutter for high-speed machining [17]. In these long cutting tool cases, other solutions such as TMD, which require additional mass, are not feasible due to the high weight of the cutting tool itself, limited by the restrictions of the spindle coupling, automatic tool changer, and tool storage. For example, with HSK-A63 clamping, there is typically a maximum weight limit of 8 kg, which could be even lower depending on the machine-tool manufacturer [38].

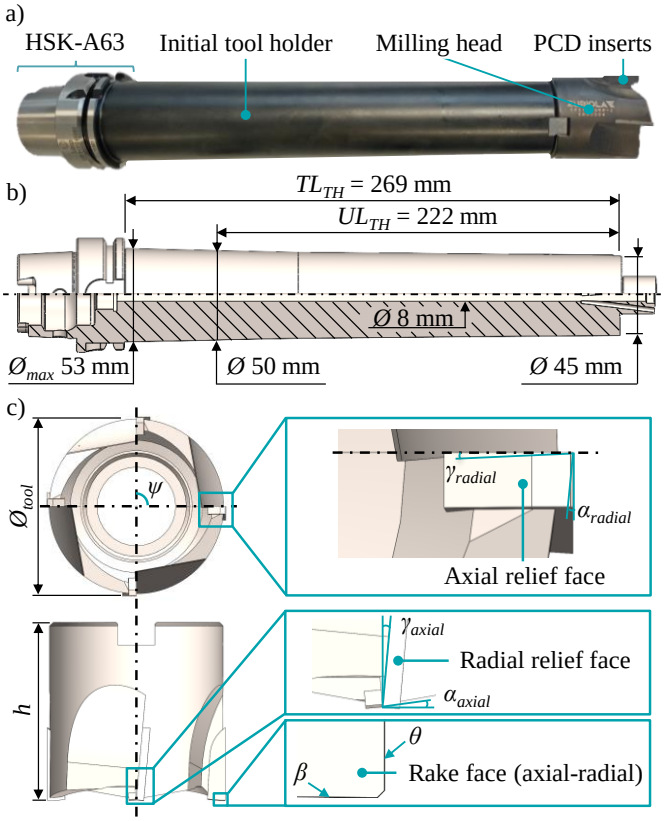

Figure 4: Case study: a) Initial cutting tool set description, b) initial tool holder design, and c) milling head cutting geometry.

The optimisation of the cutting tool set was focused on the tool holder, as it was the component that most contributes to the dynamic behaviour and could be significantly optimised due to its dimensions. To allow for a direct comparison, the same milling head was used with the initial and the optimised tool holder. The initial design of the tool holder with the most relevant dimensions for its optimisation is shown in Figure 4b. The usable length (UL_{TH}) and the total length (TL_{TH}) of the tool holder were design constraint that were maintained during the optimisation process. The usable length was the maximum depth at which the tool holder could be used with the selected milling head ($Ø_{tool}$ = 50 mm and h = 50 mm) without collisions in 3-axis machining (in this case, UL_{TH} = 222 mm). The HSK-A63 coupling cannot be modified due to DIN 69893 standard restrictions. In addition, following this standard the maximum diameter of the tool holder cannot exceed 53 mm in the HSK-A63 coupling. Internally, the initial design includes an 8 mm diameter hole for coolant supply. The rest of the remaining material volume was susceptible to optimisation.

The cutting geometry of the milling head required for specific cutting forces is detailed in Figure 4c. The cutting geometry was measured with an optical profilometer Alicona IFG4. The measurements were conducted using a 10x magnification objective with a vertical resolution of 500 μm and a lateral resolution of 3 μm to ensure accuracy (Table 1). Throughout the entire study, the defined process involved face milling with a complete tool diameter radial depth of cut of 50 mm. The selected workpiece material was a typical aluminium-silicon alloy A-356, widely employed in automotive components [3], [39]. The tool holder and milling head for both the initial and optimised designs were made of F1580 (20NiCr4) case-hardening steel according to the standard UNE36-013-76 [40]. The material properties used in this study are presented in Table 1.

Table 1: Cutting geometry and cutting tool set material properties.

Cutting geometry	Symbol	Value
Tooth angle (º)	ψ	90
Cutting edge radius (μm)	r	6
Radial rake angle (º)	γ_{radial}	0
Radial relief angle (º)	α_{radial}	10
Axial rake angle – helix angle (º)	γ_{axial}	5
Axial relief angle (º)	α_{axial}	7
Axial edge angle (º)	β	0.5
Lead angle (º)	θ	0
Material properties - F1580 steel [40]		
Density (kg/m^3)		7800
Young's modulus (GPa)		210
Poisson's ratio (-)		0.28

3.1. Design optimisation

The optimisation objective for the initial tool holder design was to maximise the natural frequency without compromising stiffness, enabling higher cutting speeds without chatter. This objective was derived from preliminary sensitivity analysis, which identified natural frequency as the most influential factor for spindle speed (higher natural frequency enhance stability at higher speeds) while stiffness primarily impacts the depth of cut, with lower stiffness reducing stable cutting depths. Increasing the stable spindle speed enables higher Material Removal Rates (MRR) without raising cutting forces, which, in the defined case study, is the preferred option. An increase in cutting forces could lead to other issues, such as elastic deformations, distortions, and forced vibrations, negatively affecting the machining process.

3.1.1. Topology optimisation

The topology optimisation was conducted using Altair Inspire 2021.1 software, chosen for its advanced optimisation features, including symmetry planes, which are essential for components like cutting tools that require precise balance around the rotation centre. The optimisation process utilised the Solid Isotropic Material with Penalisation (SIMP) method in combination with the Method of Feasible Directions (MFD) algorithm. The SIMP method, as implemented in Inspire software, defines pseudo-material density as the design variable and applies a power-law penalisation to the stiffness-density relationship, pushing the density towards a binary 0/1 (void/solid) distribution. The MFD algorithm, iteratively refines the design, enhancing the objective function while ensuring compliance with the specified constraints at each step. The topology optimisation process for the tool holder is outlined in the following main steps (Figure 5):

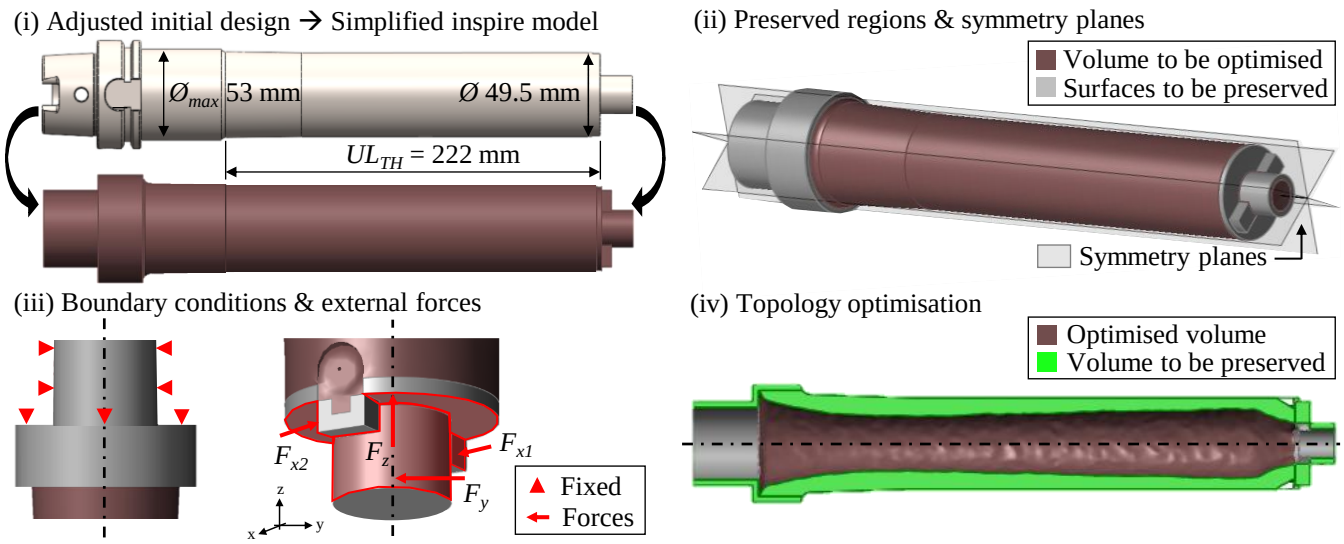

Figure 5: Topology optimisation process of the tool holder.

(i) Topology optimisation redistributes material within a defined volume but cannot increase the initial volume by adding material. Threfore, the initial design was adjusted to meet the design constraints and take full advantage of the optimisation. The design constraints for topology optimisation included the previously mentioned UL_{TH}, TL_{TH}, and HSK-A63 coupling constraints (Figure 4b). As part of the initial design adjustment, the external diameter was increased to 49.5 mm to maximise stiffness while adhering to the milling head diameter constraint. At the same time, the maximum diameter of the HSK-A63 coupling, set at 53 mm, was extended up to the UL_{TH}. For the Inspire model, the adjusted initial design of the tool holder was simplifiying certain areas, such as the clamping section of the HSK-A63, to reduce computational costs. Additionally, internal holes were removed to facilitate the optimisation process.

(ii) In the topology optimisation model, the volumes designated for preservation and optimisation were defined. Specifically, the milling head coupling surfaces and the HSK-A63 clamping surfaces were chosen for preservation and all the rest of the model was set as optimisable. Symmetry planes were employed to ensure a balanced material distribution in the redesign process.

(iii) The boundary conditions and the forces that the tool holder needs to withstand were defined. In this case, the boundary conditions of the spindle clamp were applied, constraining the displacements and rotations in the HSK-A63 doble-contact faces. In addition, the resultant cutting forces were considered in the optimisation. As the milling head was not included in the analysis, the resultant forces supported by the tool holder were applied in the milling head clamping surfaces. The resultant cutting force in the tool holder (F_x) was applied in the clamping supports in the same cutting direction. The resultant feed force (F_y) was applied radially on the coupling rod, while the vertical force (F_z) was applied on the milling head support. The applied forces' values were insignificant, as stiffness and natural frequency are structural properties unaffected by the magnitude of applied forces, relying on the geometry, material properties, and boundary conditions [41].

(iv) The topology optimisation simulation was performed. The selected simulation procedure was of "maximise stiffness" with frequency constrain for maximum natural frequency. The reference mass reduction target was stablished at 30%. The selected minimum element size in the model was of 0.5 mm, recommended by the software. Finally, the obtained result shows the material volume to be removed and the optimal material layout shape for the defined objectives. The required computational time for the simulation was 16 hours on an HP Z840 workstation with 256 GB of RAM.

The topology-optimised design suggests a material layout concentrated in the external part of the tool holder and near the spindle coupling zone (highlighted in green in Figure 5). Hence, the material needs to be reduced from the inside part of the tool holder to reduce weight and increase the natural frequency. However, this design, as it stands, cannot be manufactured through conventional machining processes. Therefore, a redesign was necessary to account for manufacturing constraints while maintaining the material layout as closely as possible to the topology optimisation results.

3.1.2. Redesign for manufacturing

The topology optimised design was redesigned according to the manufacturing constraints. In this case study, machining processes were selected for the optimised design manufacturing, but additive or hybrid processes could also be employed in other designs. In order to replicate the internal geometry of the tool holder as faithful as possible to the topology optimised shape, the tool holder was divided into two parts (Figure 6a). This approach allowed the machining (drilling and boring) of the internal geometry from the milling head side. After machining, the tool holder body (Part I) was assembled to the milling head coupling part (Part II) ensuring a run-out equal to the initial design (< 10 µm).

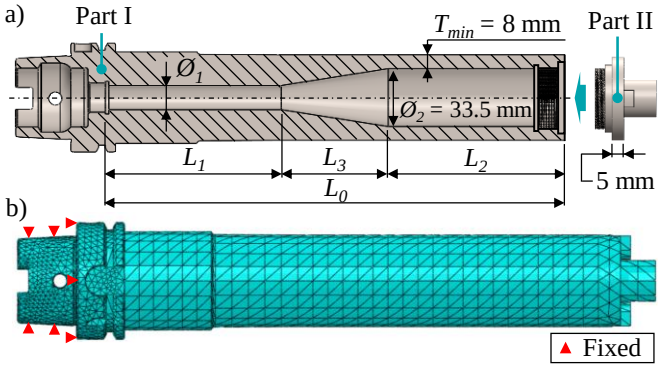

Figure 6: Redesign: a) Parameters for the redesign of the optimised tool holder, b) FEM model for natural frequency calculous.

The redesigned internal geometry consists of two diameter holes ($Ø_1$ and $Ø_2$) connected by a cone (Figure 6). This geometric configuration was the most effective approach for enabling the manufacture of the topology-optimised design. To maximise the tool holder's natural frequency, the redesign geometry was parameterised for subsequent optimisation through FEM simulations. The fixed and variable design parameters of the redesigned shape are shown in Table 2. Some dimensions were constrained by manufacturing or design requirements; the total length (L_0) of the tool holder Part I was of 264 mm, so the length of the cone (L_3) was in function L_1 and L_2. To ensure both the feasibility of manufacturing the thread to attach Part II and to prevent the wall from becoming too thin, this thickness (T_{min}) was set to 8 mm. As a result, $Ø_2$ of 33.5 mm was defined, since diameters smaller than this reduced natural frequencies. The remaining variables defining the internal geometry were subject to optimisation. Different values for L_1, L_2, *and* $Ø_1$ were tested to determine the optimal combination.

Table 2: Tool holder interior geometry redesign parameters.

	Parameter	Values
Fixed	L_0 (mm)	264
	$Ø_2$ (mm)	33.5
	T_{min} (mm)	8
	L_3 (mm)	$L_3 = L_0 - L_1 - L_2$
Variables	L_1 (mm)	5, 20, 40, 60, 80, 100, 120, 140
	L_2 (mm)	50, 75, 100, 125, 150, 175, 200
	$Ø_1$ (mm)	10, 14, 20, 24

FEM simulations were conducted to determine the optimal geometry of the redesign according to the objective of maximising the natural frequency. Simulations with different tool holder redesign dimensions were conducted in Abaqus CAE, employing the standard implicit solver (the model is shown in Figure 6b). The tool holder was modelled as a single part, assuming completely rigid joints between the two parts. Natural frequencies were calculated by "linear perturbation" procedure to obtain frequency of the first vibration mode. The employed mesh elements were tetrahedral, using a free meshing technique and the software's default algorithm. A finer mesh size of 2 mm was applied to the HSK-A63 part, while a bigger mesh size of 8 mm was used for the rest of the tool holder. Curvature control was set to 10% of maximum deviation, with a minimum size factor of 10%. The applied boundary conditions consist of constraining the displacements and rotations in all directions (fixed) on the HSK-A63 double-contact faces (Figure 6b). Although it is demonstrated later in this paper that it is not the most accurate model for quantifying real modal parameters; it was considered as a good option for qualitatively determining the best design option with relatively fast simulations. The selected material inputs were those for the tool holder F1580 steel (Table 1). A total of 102 simulations were conducted varying the dimensional parameters of L_1, L_2, and $Ø_1$.

3.2. Virtual modal analysis

Virtual modal analysis aims to predict the modal parameters of cutting tool designs necessary for their dynamic validation. The analysis focuses on the dominant vibration mode of the cutting tool, which, for long cutting tools, is clearly identified as the critical bending mode at the tool's natural frequency. Accordingly, the cutting tool assembly was modeled as a single-degree-of-freedom system to predict chatter. In the case study, the natural frequencies (ω_n) and stiffnesses (k) of both the initial and optimised cutting tool sets were predicted using FEMA.

In this work, an improved FEMA model was developed to enable efficient simulation of large cutting tool designs, providing higher accuracy while maintaining affordable computational and development costs. The model aimed for a higher fidelity representation of the cutting tool's real behaviour by considering the clamping mechanism between the spindle and the tool. Based on the hypothesis that in large cutting tools the clamping mechanism is the most influential factor, as the spindle is much stiffer than the tool itself, the spindle can be neglected in the model. The improved FEMA model was also compared to other previously developed models. As noted in the introduction, no generalised FEMA model for cutting tool modal analysis has been established in the literature, neither for the HSK-A63 tool holder. Among these models, one extended approach is to

constrain the contact surfaces of the clamping [24], [26]. However, this basic FEMA model was considered oversimplified, as it only accounts for boundary conditions at the contact area of the tool holder, neglecting the clamping mechanism. Both models were evaluated using the initial and optimised cutting tool set designs and validated through EMA. In addition, the validation was conducted on two different machine-tool spindles to verify the hypothesis that, in large cutting tools, the influence of the clamping mechanism outweighs the influence of the spindle.

Furthermore, it has been mentioned that analytical approaches are not valid because they are not feasible for complex geometries, such as the ones expected from topology optimisation. To validate this hypothesis, analytically predicted modal parameters for both designs were also compared. The employed analytical model was one of the most extended approach of Euler-Bernoulli cantilever beam (equation (1) and (2)) with a constant circular cross-section. The material properties used were those of the FEMA models (Table 1).

$$k = \frac{F}{\delta} = \frac{3 \cdot E \cdot I}{L^3} = \frac{3 \cdot E \cdot \pi \cdot Ø^4}{L^3 \cdot 64} \quad (1)$$

$$\omega_n = \sqrt{\frac{k}{m_{eff}}} = \sqrt{\frac{E \cdot Ø^2}{\rho \cdot 16}} \cdot \frac{1}{2\pi} \cdot \left(\frac{k_i}{L}\right)^2 \quad (2)$$

where, δ is the deformation, F is the force, E is the Young's modulus, I is the moment of inertia, ρ is the density of the material, m_{eff} is the effective mass, k_i is the factor that depends on the vibration mode (for the first mode k_1 = 1.875).

The FEMA models were developed in Abaqus CAE employing its “standard” configuration with implicit solver. In both models, cutting tool set was modelled as a single part, assuming fully rigid joints. The simulations were run on the same workstation used in topology optimisation using in this case 28-core parallelisation. To calculate the defined output parameters the next procedures were used:

- Natural frequencies (ω_n) were calculated using the “linear perturbation” procedure type and with the “frequency” calculation method stablishing the calculous of the first 10 frequencies. Specific boundary conditions for each model were applied during the natural frequency calculations.
- Stiffnesses (k) were calculated using a "static" procedure. This involved applying an external force (F) of 1000 N in y-direction at the milling head tip of both models (Figure 7). The deformations caused by the applied force were calculated in the same direction, and the stiffness was determined dividing the force (F) by the resulting displacements in the force direction (U_y): $k = F / U_y$.

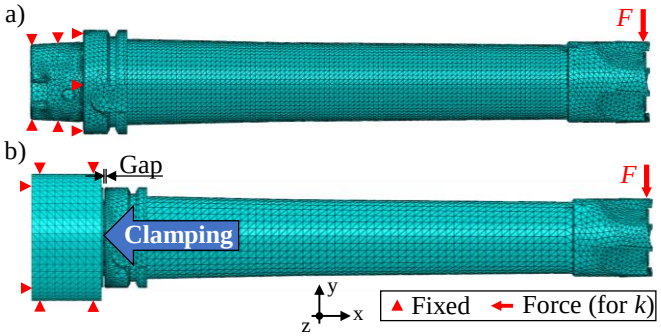

Figure 7: Modal analysis: a) Basic FEMA model, and b) Improved FEMA model.

The basic FEMA model is the simplest approach, consisting solely of the cutting tool set with boundary conditions applied to the clamping area as done in [24], [26]. The boundary conditions involved fixing the tool holder HSK-A63 double-face contact surfaces, by constraining the displacements and rotations in all directions (fixed) (Figure 7a). The used meshing elements were tetrahedral to accommodate effectively to the tool geometry, with an approximate global size of 3 mm with a maximum deviation factor of 10% between the high and the length, with a minimum size factor of 10%. The meshing size has not been considered critical in this model because the results remain constant within a reasonable size and the simulation time is reduced. In defined steps, linear analysis procedure was employed due to no nonlinearities were expected.

The developed improved FEMA model is a high-fidelity approach that simulates the clamping mechanism from an initial non-contact state to the final double-face contact (Figure 7b). This approach accounts for the mechanical loads given in the clamping of the cutting tool to the spindle coupling, ensuring a more realistic representation compared to any other model reported in the literature. In the model, the spindle is fixed while the cutting tool set is initially positioned with a 0.5 mm gap where no contact occurs. Subsequently, the clamping force ($F_{clamping}$) is applied to the internal chamfer of the cutting tool set coupling, where in reality, the collet engages due to the force actuated by the draw bar (Figure 8a). $F_{clamping}$ was applied at a reference point (RP) as a concentrated force in the x-direction, and joined to the coupling surface of the internal chamfer to maintain the force component in the same direction (Figure 8b). The clamping force for HSK-A63 type clamping has a nominal value of 18 kN, which was validated using the Power-check II device from OTT (ref. 95.103.136.9.2) in the machine tool used in experimental validation tests.

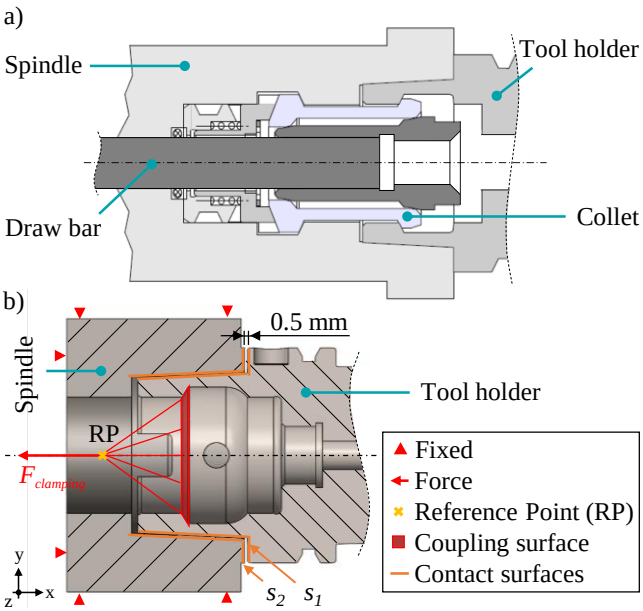

Figure 8: Improved FEMA model detailed description: a) real HSK-A63 clamping mechanism, and b) developed model configuration.

Within the improved FEMA model, a first step was defined to conduct the initial clamping simulation. Once the clamping process was completed, the natural frequency and stiffness of the tool holder could be simulated. The interaction between the spindle (s_1) and tool holder (s_2) surfaces were defined (Figure 8b). Surface to surface contact was defined for both surfaces with a constrained normal behaviour to avoid the surfaces enter into each other, and with a penalty tangential behaviour with 0.3 friction coefficient (average value for steel-to-steel contacts [42]). Within the interactions automatic smoothing of 3D geometry option was used to avoid geometrical errors at the surface contacts. To facilitate the clamping simulation, the contact control option was used with automatic stabilisation configuration.

The meshing in the improved model was more relevant than in the basic model because the simulations are more demanding due to surface contacts. Therefore, a mesh size sensitivity analysis was conducted, comparing the simulation time with the accuracy of the results. At the interaction surfaces, mesh sizes from 1.5 mm to 3.5 mm were tested, while maintaining a mesh size of 5 mm for the rest of the model. Curvature control was implemented with a maximum deviation factor of 10% between the high and the length, with a minimum size factor of 10%. The results of the meshing analysis, along with the outcomes obtained from both FEMA models for the initial and optimised designs, are validated later through EMA tests.

3.3. Virtual dynamic validation

Virtual dynamic validation involved predicting the chatter behaviour of initial and optimised cutting tool designs to quantify improvements in MRR through SLD and validate the optimised designs before manufacturing. The dynamic model for long cutting tool cases focused on the critical vibration mode, using the predicted modal parameters to predict chatter within a single-degree-of-freedom system. SLDs were calculated using two primary frequency domain models, the Average Tooth model and the Fourier Series model commonly applied in conventional machining processes such as face milling [11]. These models were compared and experimentally validated to determine the most accurate and efficient model for the virtual design methodology. The input parameters for the SLD calculations in the case study were defined as follows:

i) The cutting tool's modal parameters were predicted from the improved FEMA model within the virtual modal analysis.

ii) The required specific cutting forces, including the resultant specific cutting force (K_s) and the force orientation angle (β_0), which represents the relationship between the radial and tangential specific cutting forces, were calculated for the defined case study and workpiece material. Axial specific cutting forces were excluded from the chatter models, as the critical modes of the cutting tool involve bending in the radial plane. An empirical database for the same workpiece material (A-356), developed by Lazkano et al. [3], was employed to predict cutting forces based on empirical data from orthogonal machining tests, which were transformed to oblique cutting using the orthogonal-to-oblique transformation methods developed by [43] and [44]. From this database, shear stress (τ_s), chip compression ratio (r_c), and friction angle (β_f) were obtained for this case specific input parameters of feed per tooth (f_z), rake angle (γ), relief angle (α), and cutting edge radius (r). These input parameters were derived from the geometry of the milling tool's radial cutting edge (Table 1), using a feed per tooth value of 0.1 mm/tooth, consistent with the values used in both dynamic analysis and experimental machining tests. The obtained resultant specific cutting force was K_s = 1078 N/mm^2 with a force angle of β_0 = 62º.

iii) The process parameters for the SLDs were defined for the selected face milling operation, with a radial depth of cut equal to the milling head diameter and a cutting angle ranging from 0º to 180º.

iv) Other geometric characteristics, such as the cutting teeth, tooth passing angles, and additional parameters, were also defined in Table 1. With the predicted SLDs, stable and chatter-free cutting conditions can be established to quantify improvements in MRR and validate the developed designs before manufacturing.

The validation criterion, illustrated in Figure 9, identifies the maximum Material Removal Rate (MRR_{max}) achievable at a specific depth of cut for each cutting tool design. MRR_{max} is directly influenced by spindle speed (as shown in Equation 9), which is increased by the enhancement of the cutting tool's natural frequency through topology optimisation. The maximum stable spindle speed (S_{max}) for a given depth of cut can be identified in the stability lobe limit for both the initial and optimised designs, enabling a quantitative comparison of their productivity ($MRR_{max\ initial}$ vs. $MRR_{max\ optimised}$). Simultaneously, a maximum a_p can be established to avoid excessive cutting forces, tool and workpiece deformation, and shape errors. In addition, the limit depth of cut ($a_{p\ lim}$) directly related with the cutting tool's stiffness can be identified. This analysis quantifies the performance improvement and enables the virtual validation of the developed designs.

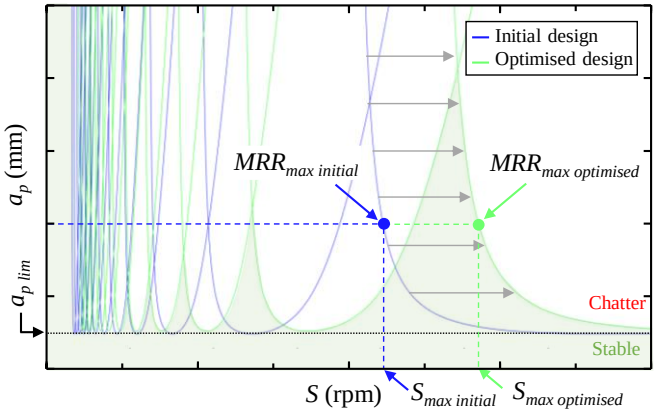

Figure 9: Dynamic validation criteria and MRR_{max} for a given a_p.

$$MRR_{max} = a_p\, a_e\, S_{max}\, f_z\, N_t \qquad (9)$$

3.4. Experimental validation procedure

The virtual design methodology was validated through Experimental Modal Analysis (EMA) and machining tests conducted with both the initial and optimised tools. The developed FEMA model was validated using EMA on different machine-tool spindles, to confirm the hypothesis that, in modelling large cutting tools the clamping is the most influential factor independent of the spindle. For the EMA, tap testing was performed on two spindles with the same HSK-A63 clamping system: (i) a Lagun L1000 (the same machine tool used for machining tests) and (ii) a GF Mikron P800. These spindles represented two distinct machine types, one from a newer 5-axis machine and the other from an older 3-axis machine. During tap testing, the cutting tool was struck with an impact hammer (Brüel & Kjaer Type 8206) to measure the excitation force, while the resulting response was recorded using an accelerometer (Brüel & Kjaer Type 4525-B). In both cases, the spindle height tested matched the requirement for the machining tests. While the machines were entirely different and not directly comparable, it was suitable for the intended comparison. The experimental set-up for EMA in Lagun L1000 is described in Figure 10a, the same equipment was used in the GF Mikron P800. Measurements in two radial directions (x and y) were performed for each cutting tool set, with three repetitions carried out for each case to ensure the robustness of the results. From the measured FRFs critical mode, experimental modal parameters of ω_n, k, and ζ were calculated following the approach described by [8]. The experimental input and output parameters for the EMA are summarised in Table 3.

In experimental machining tests, output parameters were analysed to detect chatter under different cutting conditions using both initial and optimised cutting tool sets. These tests allowed for the validation of the calculated SLDs by confirming that the predicted stable and chatter cutting conditions were indeed accurate. The experimental set-up is described in Figure 10, where face milling tests were conducted on A-356 workpiece material using a Lagun L1000 machining centre. During machining process (in-process) the measured output parameters were: (i) cutting forces (F_x, F_y, and F_z) measured through the workpiece by the Kistler 9139AA, (ii) sound emissions captured by a Brüel & Kjaer Type 4189-A-021 microphone, and (iii) accelerations (A_x, A_y, and A_z) in the spindle monitored by a triaxial accelerometer (PCB Piezotronics J356A45). Post-process, the machined surface finish was analysed measuring the surface roughness using a Mitutoyo surftest sj-210 (R_a, R_t, and R_z) as it is shown in Figure 10. This way, the whole machining system affected by chatter was comprehensively covered.

Face milling tests with a full radial depth of cut (a_e = 50 mm) were conducted at the most relevant spindle speeds and depths of cut, within the stability lobes of maximum productivity, to analyse stable and chatter behaviours. Tests that did not yield additional information were skipped to preserve cutting edges. The established spindle speed range was from 2000 to 6000 rpm with the initial design and up to 7000 rpm with the optimised design, covering a depth of cut ranging from 0.25 mm to 2 mm. A constant feed per tooth of 0.1 mm/tooth was maintained in all the tests, as chatter is independent of this parameter [8]. The good condition of the PCD inserts was ensured throughout all tests by verifying every 10 tests that there was no wear or damage to the cutting edges using a Leica Z16 APO optical macroscope. In total, 101 tests were conducted, 52 with the initial tool holder and 59 with the optimised tool holder. The complete experimental plan and cutting conditions are described in Table 3.

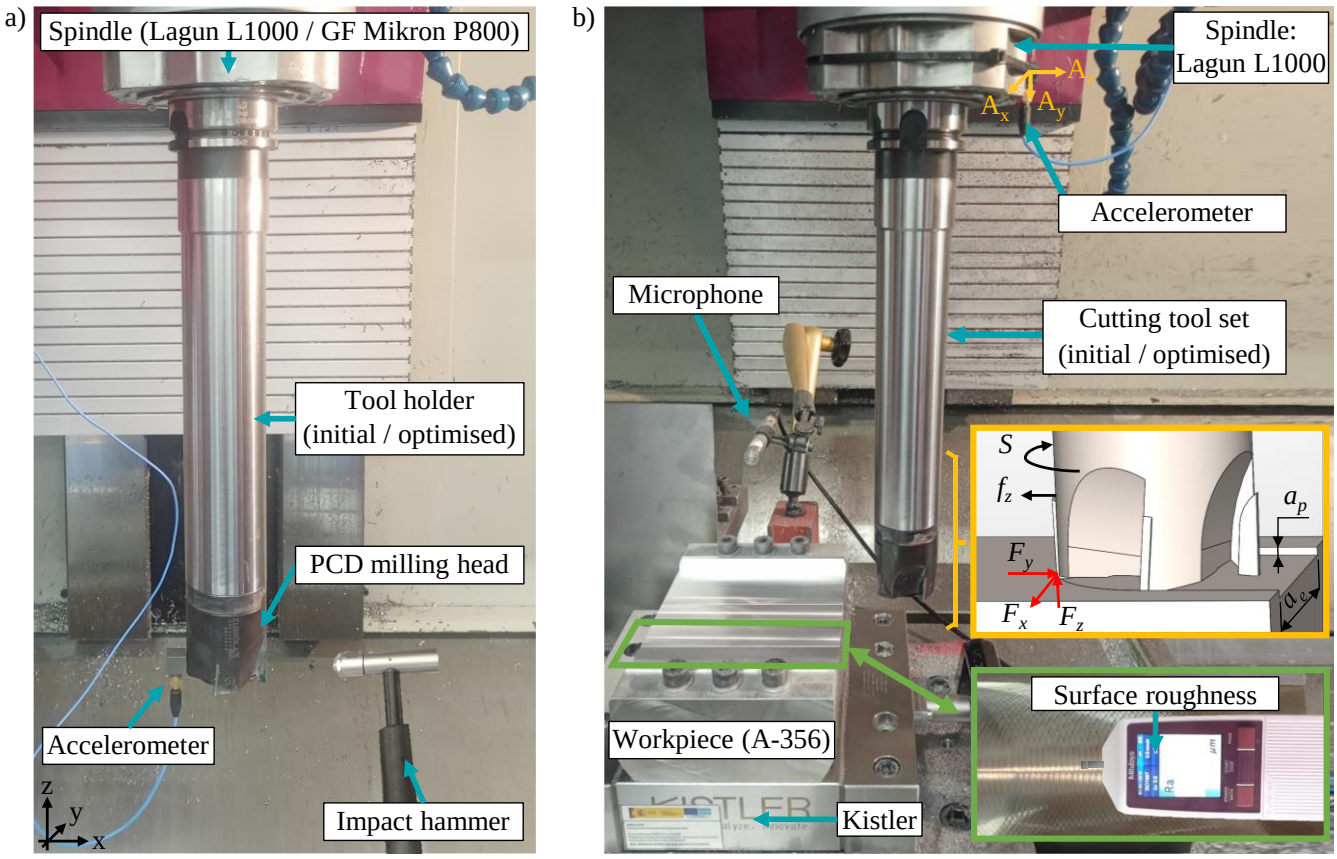

Figure 10: Experimental validation: a) EMA set-up, and b) machining tests experimental set-up.

The criteria used in the experimental tests to identify chatter was defined as follows: Chatter in cutting forces was identified by significant variations, with peak values exceeding those observed during stable machining. For accelerations and sound emissions, time-domain measurements were converted to the frequency domain using Fast Fourier Transform (FFT) to examine machining frequencies. Stable machining exhibited only the tooth passing frequency ($Freq_{tooth}$), whereas chatter was characterised by the predominance of the chatter frequency ($Freq_{chatter}$). Additionally, surface finish analysis involved measuring chatter marks post-process to evaluate their impact on roughness.

Table 3: Experimental tests input and output parameters.

	EMA	Machining tests
Input parameters	Tool holders - Initial design - Optimised design Machine-tool (spindle): - Lagun L1000 - GF Micron P800	Tool holders: - Initial design - Optimised design Cutting conditions: - a_p (mm): 0.25, 0.5, 1, 1.5, 2 - a_e (mm): 50 - f_z (mm/tooth): 0.1 - S (rpm): 2000 - 7000 Machine-tool: Lagun L1000 Workpiece: A-356
Output parameters	FRFs Modal parameters: - Natural frequency (ω_n) - Stiffness (k) - Damping (%)	In-process: - Cutting forces: F_x, F_y, and F_z - Accelerations: A_x, A_y, and A_z - Sound emissions Post-process: - Surface finish: R_a, R_t, and R_z

4. Results and discussion

Results obtained from the virtual design methodology and its experimental validation within the case study were analysed.

4.1. Design optimisation results

The topology-optimised tool holder was redesigned according to the manufacturing constraints and adjusted for maximum natural frequency through the defined FEM simulations (Figure 11a). The influence of the established design parameters L_1, L_2, and $Ø_1$ on the natural frequency can be analysed in Figure 11b. In the analysis, the resolution of the results was increased where the natural frequency was higher (in $Ø$ = 14 mm), thereby enhancing precision in the range of interest and reducing the time required by avoiding unnecessary simulations. Finally, the optimum redesign geometry for maximising the natural frequency was obtained: L_1 = L_2 = 100 mm, and $Ø_1$ = 14 mm. The developed redesign enables the manufacturing of the optimised tool holder as faithful as possible to the geometry suggested by the topology optimisation.

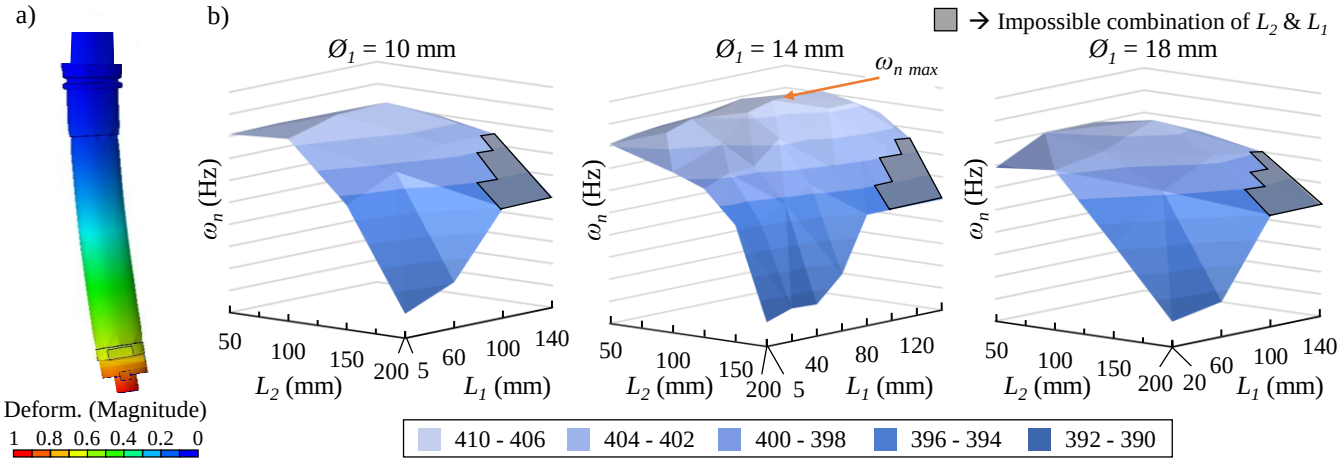

Figure 11: Redesign optimisation results: a) FEM model result example, and b) natural frequency results for different parameters.

Once the optimised design was defined and virtually validated, the optimised tool holder was manufactured (shown in Figure 10). In the manufacturing process, an acceptable run-out was ensured (the same as the initial cutting tool set, under 10 µm) as well as correct balancing using Haimer's modular balancing machine (TD103-H01-EU) to achieve a balancing quality grade under 2.5 at 10000 rpm. In terms of weight reduction, the optimisation achieved a 16% reduction; the initial design weighed almost 5 kg, whereas the optimised design weighed 4.3 kg. The lightweighting also contributes to significant improvements by reducing the stress that machine-tool components such as spindle bearings, automatic tool changers, and storage need to withstand. However, the crucial factor for dynamic behaviours was not just the weight reduction but also the optimised weight distribution achieved through topological optimisation, which is reflected in the modal parameters.

4.2. Virtual modal analysis validation

The developed FEMA model results for the virtual modal analysis of the cutting tool designs and its experimental validation through EMA tests are described below.

4.2.1. FEMA model results

As part of the development of the improved FEMA model, a mesh size analysis of the clamping area was conducted. Figure 12a illustrates the relationship between mesh size, simulation time, and average error (calculated for stiffness and natural frequency) compared to experimental results. This analysis was first performed on the initial design and then applied to the optimised design. The analysis concluded that a 2 mm mesh size provided the optimal balance between computational time and accuracy, delivering precise results within 2 hours. It was also observed that mesh sizes greater than 3 mm failed to achieve full clamping of the cutting tool (no double-face contact), while mesh sizes smaller than 1.5 mm stabilised the error but significantly increased computational time without any notable improvements. Figure 12b presents the improved FEMA model's clamping simulation with the optimised mesh size. The initial and final clamping states, along with the corresponding equivalent von Mises stresses, are shown. The stresses are primarily concentrated in the conical region where the force is applied, and contact between the spindle and cutting tool faces occurs. Ultimately, the double-face contact of the HSK-A63 was successfully simulated.

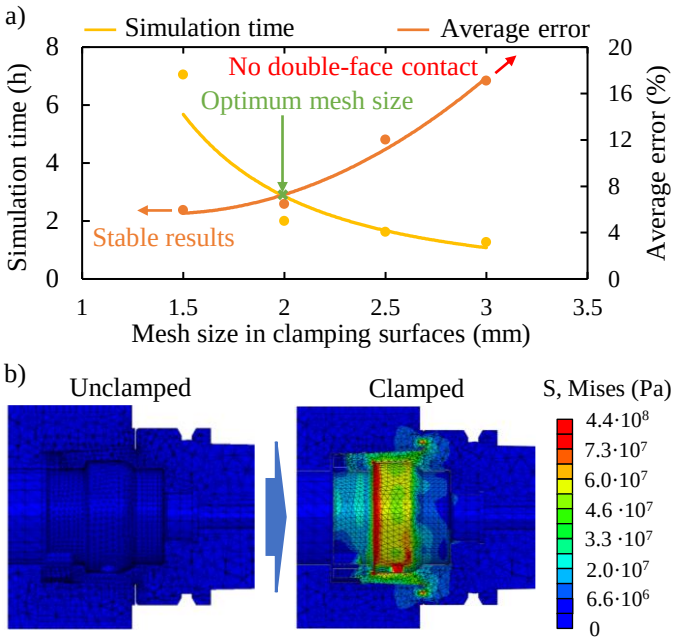

Figure 12: Improved FEMA model: a) mesh size analysis in the initial design, and b) clamping simulation results.

The modal parameter results for the initial and optimised tool designs obtained from the improved FEMA model and the basic FEMA model are presented in Table 4. A comparison reveals that the stiffness and natural frequency values predicted by the basic FEMA model are higher than those from the improved FEMA model, highlighting significant differences when the clamping mechanism is simulated. The boundary conditions in the basic model appear overly restrictive, as the clamping mechanism does not function as a welded joint. In both models, as anticipated, the natural frequency of the cutting tool set increased with the optimised design. Additionally, the objective of maintaining stiffness was met, with a slight increase attributed to the external shape adjustments made prior to topology optimisation.

Table 4: Virtual modal analysis with basic and improved FEMA models.

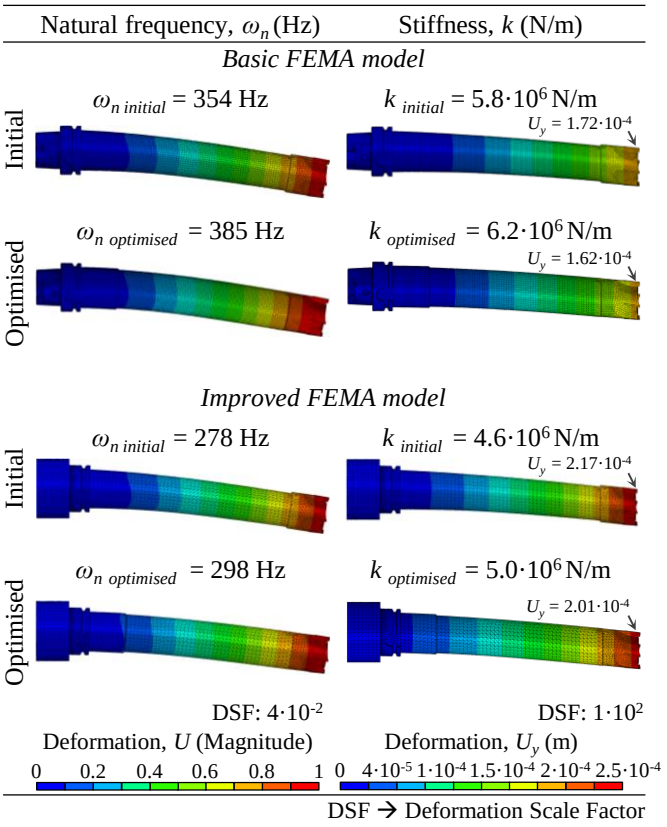

4.2.2. FEMA model validation

To validate the developed FEMA model, the predicted modal parameters were compared with experimentally measured values obtained by evaluating the cutting tool's FRFs through EMA, conducted on two machine-tool spindles and cutting tool designs. Figure 13a illustrates the experimental FRFs for the initial and optimised tools in both spindle I (Lagun L100) and spindle II (GF Mikron P800), alongside the FRFs reconstructed using the predicted modal parameters from the improved FEMA model. In the FRFs, the dominant vibration mode at the cutting tool's natural frequency is clearly identifiable, validating the approach of focusing the analysis on this single dominant vibration mode. Comparing the FRFs from both machine-tool spindles confirmed the initial hypothesis that, in the virtual modal analysis of large cutting tools, the spindle's significantly higher stiffness minimises its influence on the cutting tool dynamics. The FRFs in the critical mode were nearly identical between the two spindles, with natural frequencies differing by less than 1 Hz, and spindle II showing slightly higher stiffness. While minor differences were observed in other regions of the FRFs, corresponding to modes attributed to the spindle, these differences were negligible within the scope of the described modal analysis.

Comparing the measured FRFs of the initial and optimised cutting tools revealed that the optimised design achieved a higher natural frequency (Figure 13a). Experimental modal parameters extracted from spindle I FRFs (the spindle used in machining tests) were compared with the predicted values, as shown in Figure 13b. The results demonstrate that the design optimisation increased the natural frequency from 265 Hz to 286 Hz, representing an 8% improvement, which significantly enhances chatter stability in machining dynamics. While the stiffness of the optimised design was expected to be maintained or slightly increased, the actual measured stiffness (4.7 N/μm) was slightly lower than that of the initial design (4.9 N/μm), likely due to the binding effect between the two parts of the optimised tool holder (Figure 6). The measured damping in both cases aligned with the reference value of 3% used in SLD prediction but was slightly higher in the optimised tool (3.5%) compared to the initial tool (2.5%), also attributed to the binding effect in the tool holder assembly.

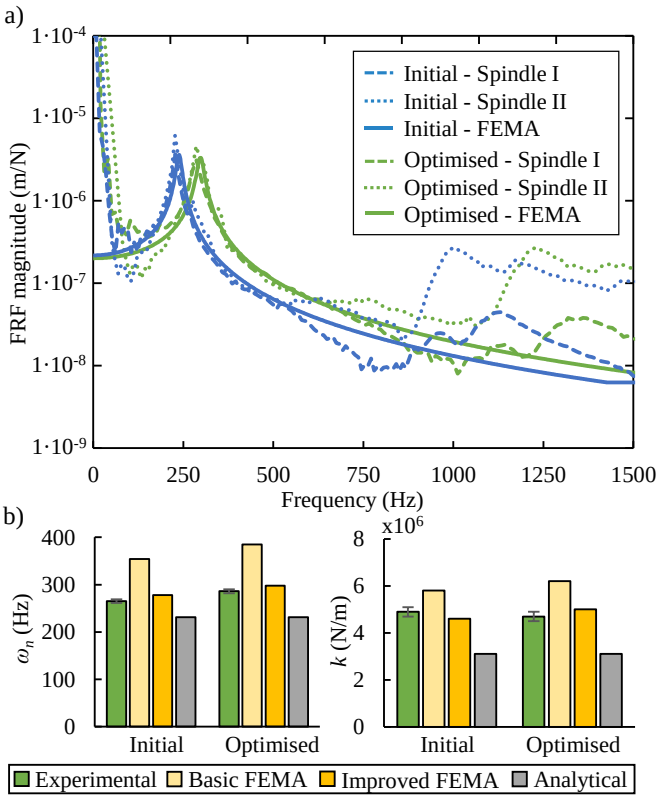

Figure 13: Improved FEMA model validation: a) FRF comparison, and b) modal parameters comparison.

The improved FEMA model was initially validated by comparing the predicted results with experimentally measured FRFs, revealing a strong correlation (Figure 13a). The predicted modal parameters were then compared with experimental data (from spindle I) as well as results from the basic FEMA and analytical models (Figure 13b). Among the FEMA models, the improved FEMA model outperformed others, achieving an average error of only 6% with an optimised computational cost of approximately two hours (Figure 12a). In contrast, the basic FEMA model, as expected, significantly overestimated the cutting tool's stiffness and natural frequencies, with an unacceptable average error of nearly 30%. Therefore, the basic FEMA model is unsuitable for accurately predicting realistic modal parameters, despite its shorter simulation and development times. In addition, results confirmed the inadequacy of the analytical approach in accurately predicting the stiffness and natural frequency of cutting tools, with an average error of 18%. This discrepancy likely arises from its inability to incorporate geometric complexities, such as internal structures, and its failure to represent the double-face contact clamping mechanism effectively.

This validation confirms that, for large cutting tools, accurately simulating the clamping mechanism is essential to improving the precision of modal parameter predictions, independent of the machine-tool spindle. The minor discrepancies observed can be attributed to the influence of the spindle structure, which can reasonably be excluded from the presented virtual design methodology, as its detailed modelling would result in inefficient development processes and increased experimental costs. In the end, the improved FEMA model has proven to be an effective and efficient solution for virtual modal analysis of large cutting tool designs, offering a balance of high accuracy and affordable computational demands.

4.3. Machining dynamic validation

The virtual dynamic validation of the cutting tool designs was completed by predicting the SLDs using modal parameters obtained from FEMA. The input parameters for the SLDs were consistent with those defined in the virtual dynamic validation process and, two principal approaches—Average Tooth model and the Fourier series model— were compared to determine the optimal method. The predicted SLDs for the initial (Figure 14a) and the optimised (Figure 14b) designs clearly demonstrate that the optimised cutting tool set enhances machining stability at higher spindle speeds. The design optimisation shifted the stability lobes to higher spindle speeds due to the increased natural frequency, thereby enabling higher MRR. The depth of cut, ($a_{p\ lim}$) remained nearly identical for both cutting tools, as stiffness was preserved during optimisation. Comparing the two approaches, the Fourier series model predicted more restrictive SLDs regarding stability compared to the Average Tooth model.

Experimental machining tests were conducted using both the initial and optimised tool sets under various cutting conditions along the predicted SLDs. During these tests, the defined output variables were measured to detect chatter and classify each cutting condition as stable or unstable (chatter). The experimental chatter results under different cutting conditions of a_p and S were overlaid on the predicted SLDs of each tool design (Figure 14). Comparing the employed models, Fourier series approach demonstrated to be able to predict chatter within a tolerance of ±125 rpm for both cutting tool designs. In contrast, the Average Tooth model consistently overestimated the stability lobes across the entire spindle speed range. Therefore, it was concluded that the Fourier series model was the best option for the developed methodology. The only discrepancies with the Fourier model were observed at a depth of cut of 0.5 mm and spindle speeds between approximately 5000 to 5500 rpm in both cutting tool designs. In this specific range, no chatter vibrations were measured, yet the model predicted chatter. These discrepancies could be due to the limitations of the chatter model itself or possible inaccuracies in the predicted input parameters, such as deviations in the specific cutting forces and the modal parameters predicted from improved FEMA model.

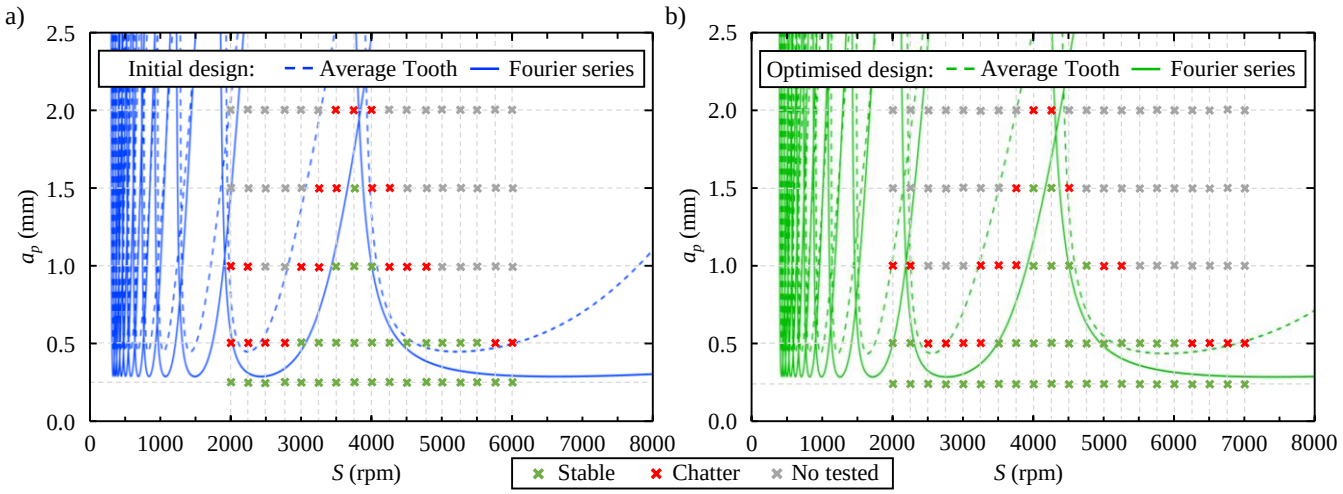

Figure 14: Experimental validation of the dynamic models for: a) initial cutting tool, and b) optimised cutting tool.

An example of experimentally measured outputs for chatter detection are shown in Table 5. Demonstrating the superiority of the optimised design, when comparing chatter condition with the initial cutting tool (S = 4250 rpm) and stable conditions with the optimised design at 500 rpm higher spindle speeds (S = 4550 rpm) in the same depth of cut of 1 mm. The effects of chatter on the measured output parameters were evident. During machining, the maximum cutting forces were three times higher, and the acceleration and sound amplitudes increased at chatter frequencies. Additionally, the machined surface roughness increased by over 35% in R_a.

Table 5: Experimental machining tests output results.

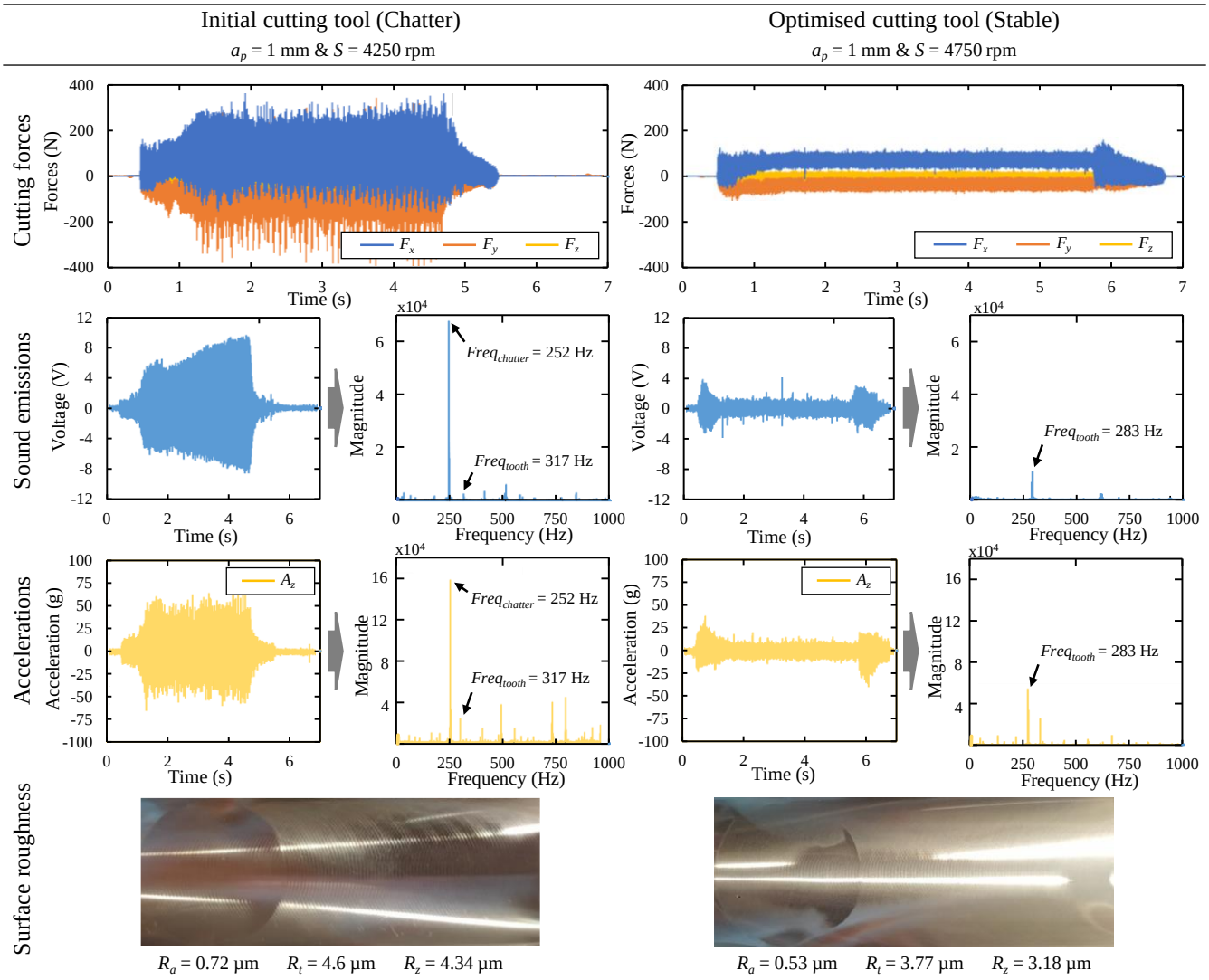

After validating the dynamic model, the performance improvements of the optimised cutting tool were quantified. The obtained improvements comparing both initial and optimised cutting tool test were analysed in terms of the obtainable maximum stable material removal rate (MRR_{max}) following the defined criteria (Figure 9) and equation (9). The MMR_{max} for the tested cutting depths (a_p) were calculated for the maximum stable spindle speed (S_{max}) within the defined cutting process. The obtained MRR_{max} results are shown in Figure 15. Results for a_p = 2 mm were not considered, as no stable conditions were found, and results for a_p = 0.25 mm were also excluded because no chatter occurred, as it was below $a_{p\,lim}$. The improvements in MRR with the optimised design were significant across all depths of cut, but especially for the depth of cut of 1 mm, where the enhancement was nearly 20%.

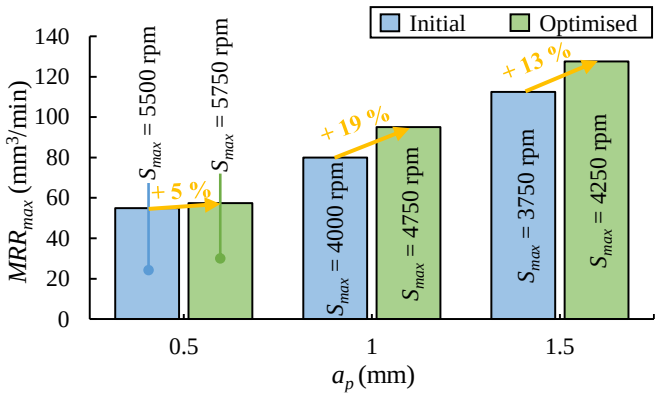

Figure 15: Initial and optimised cutting tool MRR_{max}.

5. Conclusions

A cost-effective virtual cutting tool design methodology was successfully developed and validated with a long milling tool case study. The experimental results provide robust evidences of the methodology's effectiveness in optimising large cutting tools to enhance dynamic performance and improve machining process productivity. The conclusions drawn from this study are presented below:

- The virtual design methodology effectively optimised a large milling tool set in a real case study, resulting in a 20% improvement in MRR compared to the initial design. This optimisation was achieved with reduced development costs and without the need for experimental testing, providing significant advantages, particularly for large tools. In the future, this methodology could be extended to other cutting tools, particularly those where the critical component of the machine-tool system is less stiff than the spindle.
- Topology optimisation of cutting tools can enhance stability and improve productivity within an effective design method. This was validated for the first time through a real case study and comprehensive experimental tests. Topology optimisation increased the cutting tool's natural frequency, reducing chatter at higher spindle speeds. In machining tests, the stability of the optimised cutting tool was improved by 500 rpm across various depths of cut, simultaneosuly increasing MRR.
- The improved FEMA model provided accurate virtual modal analysis of large cutting tools, enhancing the precision of previous models through a higher-fidelity approach that simulates the double-face contact clamping mechanism of the HSK-A63. In EMA tests, the improved FEMA model demonstrated an average error of 6%, significantly higher accuracy than previous basic FEMA model, with error exceeding 30% due to oversimplified boundary conditions. At the same time, the hypothesis that in large cutting tools the modeling of the clamping mechanism is more relevant than the spindle was corroborated. Additionally, it was confirmed that commonly used analytical approaches can be not suitable for predicting modal parameters, as they fail to account for double-face contact boundary conditions and complex geometric features.
- During dynamic validation, chatter was predicted with a tolerance of ±125 rpm using the modal parameters from the virtual modal analysis. The Fourier model demonstrated significantly higher accuracy than the Average Tooth model, and as a result, it was selected for the proposed methodology.

Acknowledgments

The authors hereby thank the TAILORSURF (PID2022-139655OB-I00), EVMACH (ZL-2022/00741) and ORLEGI (KK-2024/00005) projects for the financial support.

References

[1] H. C. Möhring and K. T. Werkle, “Lightweight semi-actively damped high performance milling tool,” CIRP Annals, 2022; 71: 353–356, doi: 10.1016/j.cirp.2022.04.051.

[2] Mapal, “Continuous process for electromobility” Accessed: 09, 2024, https://news.mapal.com/en-int/a/statorgehaeuse.

[3] X. Lazkano, P. Aristimuño, and P. Arrazola, “Improvement of material databases for cutting force prediction in finishing conditions of A-356 aluminium alloy,” Procedia CIRP, 2020, 122–125, doi: 10.1016/j.procir.2020.09.192.

[4] W.-K. Wang, M. Wan, W.-H. Zhang, and Y. Yang, “Chatter detection methods in the machining processes: A review,” J Manuf Process, 2022; 77:240–259, doi: 10.1016/j.jmapro.2022.03.018.

[5] A. Häusler, K. T. Werkle, W. Maier, and H. C. Möhring, “Design of lightweight cutting tools,” International Journal of Automation Technology, 2020;14: 326–335, doi: 10.20965/ijat.2020.p0326.

[6] G. Quintana and J. Ciurana, “Chatter in machining processes: A review,” 2011. doi: 10.1016/j.ijmachtools.2011.01.001.

[7] J. Munoa et al., “Chatter suppression techniques in metal cutting,” CIRP Annals, 2016; 65: 785–808.

[8] Tony L. Schmitz and K. Scott Smith, “Machining Dynamics Frequency Response to Improved Productivity Second Edition,” 2019. doi: 10.1007/978-3-319-93707-6.

[9] L. Zhu and C. Liu, “Recent progress of chatter prediction, detection and suppression in milling”, Academic Press, 2020 doi: 10.1016/j.ymssp.2020.106840.

[10] T. L. Schmitz, T. J. Burns, J. C. Ziegert, B. Dutterer, and W. R. Winfough, “Tool length-dependent stability surfaces,” Machining Science and Technology, 2004, 8: 377–397, doi: 10.1081/MST-200038989.

[11] Y. Altintas, G. Stepan, D. Merdol, and Z. Dombovari, “Chatter stability of milling in frequency and discrete time domain,” CIRP J Manuf Sci Technol, 2008; 1: 35–44, doi: 10.1016/j.cirpj.2008.06.003.

[12] P. J. Arrazola, T. Özel, D. Umbrello, M. Davies, and I. S. Jawahir, “Recent advances in modelling of metal machining processes,” CIRP Ann Manuf Technol, 2013; 62: 695–718, doi: 10.1016/j.cirp.2013.05.006.

[13] E. Graham, M. Mehrpouya, and S. S. Park, “Robust prediction of chatter stability in milling based on the analytical chatter stability,” J Manuf Process, 2013; 15: 508–517, doi: 10.1016/j.jmapro.2013.08.005.

[14] G. Li, M. Liu, and S. Zhao, “Reduced computational time in 3D finite element simulation of high speed milling of 6061-T6 aluminum alloy,” Machining Science and Technology, 2021; 25: 558–584, doi: 10.1080/10910344.2020.1855651.

[15] B. Lin, L. Wang, Y. Guo, and J. Yao, “Modeling of cutting forces in end milling based on oblique cutting analysis,” The International Journal of Advanced Manufacturing Technology, vol. 84, pp. 727–736, 2016.

[16] G. Ortiz-de-Zarate et al., “Methodology to establish a hybrid model for prediction of cutting forces and chip thickness in orthogonal cutting condition close to broaching,” The International Journal of Advanced Manufacturing Technology, 2019; 101: 1357–1374, , doi: 10.1007/s00170-018-2962-1.
[17] Y. Yang, Y. Wang, and Q. Liu, “Design of a milling cutter with large length–diameter ratio based on embedded passive damper,” JVC/Journal of Vibration and Control, 2019; 25: 506–516, doi: 10.1177/1077546318786594.
[18] C. Deng, et al., “Multi-fidelity modeling supported prediction of position and overhang length-dependent tool tip dynamics with limited labeled data,” J Manuf Process, 2024; 122, doi: 10.1016/j.jmapro.2024.05.067.
[19] T. Schmitz, E. Betters, E. Budak, E. Yüksel, S. Park, and Y. Altintas, “Review and status of tool tip frequency response function prediction using receptance coupling”, 2023; doi: 10.1016/j.precisioneng.2022.09.008.
[20] T. Schmitz, A. Honeycutt, M. Gomez, M. Stokes, and E. Betters, “Multi-point coupling for tool point receptance prediction,” J Manuf Process, 2019; 43: 2–11, doi: 10.1016/j.jmapro.2019.03.043.
[21] T. L. Schmitz, K. Powell, D. Won, G. S. Duncan, W. G. Sawyer, and J. C. Ziegert, “Shrink fit tool holder connection stiffness/damping modeling for frequency response prediction in milling,” Int J Mach Tools Manuf, 2007; 47: 1368–1380.
[22] Y. Ji, Q. Bi, S. Zhang, and Y. Wang, “A new receptance coupling substructure analysis methodology to predict tool tip dynamics,” Int J Mach Tools Manuf, 2018; 126: 18–26, doi: 10.1016/j.ijmachtools.2017.12.002.
[23] K. Kiran, H. Satyanarayana, and T. Schmitz, “Compensation of frequency response function measurements by inverse RCSA,” Int J Mach Tools Manuf, 2017; 121: 96–100, doi: 10.1016/j.ijmachtools.2017.04.004.
[24] N. Grossi, F. Montevecchi, A. Scippa, and G. Campatelli, “3D finite element modeling of holder-tool assembly for stability prediction in milling,” in Procedia CIRP, 2015; 527–532. doi: 10.1016/j.procir.2015.03.031.
[25] C. Zhou, “Research on the radial accuracy and stiffness of HSK tool system in high speed machining,” in Key Engineering Materials, 2011; 1335–1340. doi: 10.4028/www.scientific.net/KEM.480-481.1335.
[26] D. F. Tao, D. S. Zheng, J. Chen, and G. C. Wang, “Unbalance response of HSK hydraulic chuck tooling system for high-speed machining,” in Materials Science Forum, 2016; 387–393. doi: 10.4028/www.scientific.net/MSF.836-837.387.
[27] J. Wang, B. Wu, Y. Hu, E. Wang, and Y. Cheng, “Modeling and modal analysis of tool holder-spindle assembly on CNC milling machine using FEA” Applied Mech. & Mat., 2012; 220–226, doi:10.4028/www.scientific.net/AMM.157-158.220.
[28] C. Trivikrama Raju, S. Jakeer Hussain, and G. Yedukondalu, “Experimental chatter process stability using end milling process on Al6061 alloy with multiple bearing span conditions”, 2023; doi: 10.1016/j.matpr.2023.02.341.
[29] O. Özşahin, “Optimization of variable pitch milling tools for improved chatter stability,” J Manuf Process, 2024; 120: 260–271, 2024, doi: 10.1016/j.jmapro.2024.04.025.
[30] W. Ma, J. Yu, Y. Yang, and Y. Wang, “Optimization and tuning of passive tuned mass damper embedded in milling tool for chatter mitigation,” Journal of Manufacturing and Materials Processing, 2021; doi: 10.3390/jmmp5010002.
[31] M. Wang, P. Qin, T. Zan, X. Gao, B. Han, and Y. Zhang, “Improving optimal chatter control of slender cutting tool through more accurate tuned mass damper modeling,” J Sound Vib, 2021; 513, doi: 10.1016/j.jsv.2021.116393.
[32] M. Kim, J. H. Kim, M. Lee, and S. K. Lee, “Surface finish improvement using a damping-alloy sleeve-insert tool holder in the end milling process,” Int. Jour. of Adv. Man. Tech., 2020; 106: 2433–2449, doi: 10.1007/s00170-019-04757-0.
[33] P. Hanzl, M. Zetek, V. Rulc, H. Purs, and I. Zetkova, “Finite Element Analysis of a Lightweight Milling Cutter for Metal Additive Manufacturing,” Manufacturing Technology, 2020.
[34] P. Hanzl and I. Zetková, “Benefits of a New Approach to Designing Milling Cutter Using Metal Additive Manufacturing,” Manufacturing Technology, 2019; 19.
[35] D. Tomasoni, L. Giorleo, and E. Ceretti, “Milling tool optimization by topology optimization technique,” in ESAFORM 2021 - 24th International Conference on Material Forming, 2021. doi: 10.25518/esaform21.3972.
[36] T. Schmitz, G. Corson, D. Olvera, C. Tyler, and S. Smith, “A framework for hybrid manufacturing cost minimization and preform design,” CIRP Annals, 2023; 72: 373–376, doi: 10.1016/j.cirp.2023.04.051.
[37] P. Hanzl, I. Zetková, and M. Zetek, “Comparison of lightweight and solid milling cutter capabilities,” Manufacturing Technology, 2020; 20, 23–26, doi: 10.21062/mft.2020.008.
[38] Makino, “DA300 Vertical 5-Axis.” Accessed: 03, 2024. Available: https://www.makino.eu/en-us/machine-technology/machines/vertical-5-axis/da300
[39] S. Gupta, S. Abotula, and A. Shukla, “Determination of JC parameters for cast Al alloys,” J Eng Mat. Tech., 2014; 136.
[40] Ausa special steels, “Case hardening steel F1580.” Accessed: 09, 2023. Available: https://www.ausasteel.com/aceros/aceros-especiales/aceros-de-cementacion/acero-de-cementacion-f1580/
[41] Q. Xia, T. Shi, and M. Wang, “A level set based shape and topology optimization method for maximizing the simple or repeated first eigenvalue of structure vibration,” Struct. Mult. Opt., 2011; 43: 473–485, doi: 10.1007/s00158-010-0595-6.
[42] M. A. Chowdhury and D. M. Nuruzzaman, “Experimental investigation on friction and wear properties of different steel materials,” Tribology in Industry, 2013; 35: 42.
[43] R. H. Brown and E. J. A. Armarego, “Oblique machining with a single cutting edge,” International Journal of Machine Tool Design and Research, 1964; 4: 9–25, doi: 10.1016/0020-7357(64)90006-X.
[44] E. J. A. Armarego and R. C. Whitfield, “Computer Based Modelling of Popular Machining Operations for Force and Power Prediction,” CIRP Annals, 1985; 34: 65–69, doi: 10.1016/S0007-8506(07)61725-9.